Advanced Multidisciplinary Engineering Journal
AMEJ
ISSN: 3070-5797/
Journal Homepage
https://pub.scientificirg.com/index.php/AMEJ

Enhanced Multi-Generation Geothermal System for Sustainable Energy, HHO, and Freshwater Production

Ahmed Hussien[a], Ahmed Elsayeh[a], Ahmed Mostafa[a], Adham Mohamed[a], Karim Mohamed[a], Mohamed Kamal[a], Khaled Ramzy[a1], Sherin A.M. Ali[a], Mohammed Alswat[b], Walaa R. Abdelrahman[b]

[a] *Department of Mechanical Engineering, Faculty of Engineering, Suez Canal University, Ismailia, Egypt*
Emails: Ahmed10alyan@gmail.com, ahmedelsayeh360@gmail.com, sallamahmed239@gmail.com, adhammsalamma@gmail.com, km2032003@gmail.com, mohamed22kamal2233@gmail.com, kh.ramzy2005@eng.suez.edu.eg, Shireen_Mansoor@eng.suez.edu.eg

[b] *Department of Mechanical Engineering, Faculty of Engineering, University of Tabuk, 71491, Saudi Arabia*
Emails: malswat@ut.edu.sa, Wabdelrahman@ut.edu.sa

ABSTRACT

The growing demand for sustainable energy, clean water, and green fuels has increased interest in integrated renewable-energy systems, which can produce multiple valuable outputs from a single energy source. In this paper, a laboratory-scale geothermal-based multi-generation system was designed, developed, and experimentally investigated for the production of electricity, HHO gas, and desalinated freshwater. The proposed system is composed of a geothermal steam generator, a steam turbine coupled with a DC generator, an alkaline water electrolyzer, and a waste-heat-assisted solar still combined by a thermal cascading configuration. The steam turbine for electricity generation was driven by the superheated steam generated from the geothermal heat source. In order to improve the performance of the solar desalination unit, the electricity generated was then used to produce HHO using an alkaline electrolyzer, and the low-pressure turbine exhaust steam was recovered in a submerged heat exchanger. In addition, a three-dimensional Computational Fluid Dynamics (CFD) simulation was performed using ANSYS Fluent to study the fluid flow and heat transfer behavior and to validate the experimental results. The experimental results showed the stable operation of the integrated system with an average electrical power output of about 31 W, which is enough to run the electrolyzer continuously. The maximum efficiency in the four-cell alkaline electrolyzer was about 79%, and the time of HHO production was decreased compared to the two-cell. The recovered turbine exhaust heat improved desalination performance significantly with increased freshwater productivity to 8.6 L day^{-1}. Water quality analysis indicated a significant reduction of total dissolved solids (TDS) to about 76 ppm, indicating the production of high-quality fresh water. The maximum deviation between numerical and experimental results was approximately 6%. The results demonstrate the technical feasibility of integrating geothermal power generation, HHO production, and desalination on a single platform.

PAPER INFORMATION

HISTORY

Received: 3 March 2026
Revised: 30 May 2026
Accepted: 25 June 2026
Online: 27 June 2026

MSC

80M10; 80A20; 65N08; 76D05; 76R50

KEYWORDS

Geothermal Energy;
HHO;
Alkaline electrolyzer;
ANSYS Fluent;
Desalination.

[1] *Corresponding Author: Department of Mechanical Engineering, Faculty of Engineering, Suez Canal University, Ismailia, Egypt, E-mail: kh.ramzy2005@eng.suez.edu.eg*

1. INTRODUCTION

The increased environmental concerns and impacts of climate change, along with the rapid growth in global population, industrialization, and urbanization, have led to the increased demand for sustainable energy and freshwater resources. Meanwhile, the exhaustion of conventional fossil fuels and the increasing need to reduce greenhouse gas emissions have spurred the transition to renewable and low-carbon energy systems. Hence, the development of integrated technologies to simultaneously address energy, water, and environmental issues has become one of the major research priorities all over the world [1], [2]. Among the renewable energy sources, geothermal energy is recognized as one of the most reliable and sustainable energy sources due to its availability, high-capacity factor, and weather independence. Geothermal resources can provide stable base load power all year round, unlike solar and wind energy systems, making them particularly attractive for long-term energy security. However, conventional geothermal applications are generally limited to areas with naturally permeable reservoir rocks and adequate fluid circulation. Enhanced geothermal systems (EGS) have emerged as a promising technology to overcome these limitations by enabling the extraction of thermal energy from deep hot rock formations through artificially enhancing the reservoir permeability and fluid flow characteristics [3–5].

Recent advances in drilling, stimulation, and heat extraction technology have greatly expanded the potential of EGS for large-scale electricity generation and integrated energy applications. Therefore, EGS technology has attracted considerable interest as an important contributor to future carbon-neutral energy systems and sustainable energy transitions [3], [6]. Hydrogen has also attracted considerable interest as a clean energy carrier for supporting future decarbonized economies. Hydrogen produced from water electrolysis using renewable electricity, often termed green hydrogen, provides a carbon-free fuel option for transportation, industrial processes, and energy storage applications. Alkaline water electrolysis is still one of the most mature and commercially viable electrolysis technologies available, characterized by a simple construction, a long operational lifetime, a relatively low capital cost, and high operational reliability [7, 8]. Thus, coupling renewable electricity generation with alkaline electrolysis is a promising pathway for sustainable hydrogen production.

Another pressing global problem is the lack of fresh water, especially in dry and semi-dry regions where conventional sources of fresh water are limited. Desalination technologies are gaining importance to meet the freshwater demand; however, many desalination processes are still energy intensive. Solar stills are a simple and environmentally friendly way to desalinate water, especially for remote communities. However, the productivity of solar stills is usually constrained by the availability of thermal energy. Several studies have proved that coupling waste heat recovery systems to desalination units can greatly increase the evaporation rates and freshwater productivity without additional fuel consumption [1], [2]. Geothermal power generation, hydrogen production, and water desalination are technologies that have been widely studied as individual technologies, but studies that focus on their simultaneous integration in a single renewable-energy platform are limited. Most of the present studies are related to thermodynamic simulations, techno-economic evaluations, or theoretical assessments of multi-generation systems, while experimental demonstrations are relatively rare. Moreover, the literature has paid relatively little attention to the use of turbine exhaust heat for desalination enhancement and the numerical validation of integrated geothermal multi-generation systems. In order to fill these research gaps, the present study proposes and experimentally investigates an integrated geothermal-based multi-generation system for simultaneous production of electricity, HHO gas, and freshwater. The proposed system employs a thermal cascading technique, where the geothermal thermal energy is initially converted into electrical power by a micro steam turbine-generator unit. The generated electricity is then used for hydrogen production by alkaline water electrolysis, and the remaining thermal energy in the turbine exhaust steam is recovered and fed to solar still to increase the freshwater production. In addition, three-dimensional Computational Fluid Dynamics (CFD) simulations are conducted by using ANSYS Fluent to investigate the heat transfer and fluid flow characteristics and verify the experimental results. The developed system intends to maximize geothermal energy utilization, enhance the overall system efficiency, and show the feasibility of integrated renewable energy-water production for sustainable and decentralized applications.

1.1 Literature Review

Geothermal energy is one of the most reliable renewable energy resources due to its continuous availability, high capacity factor, and independence from seasonal and weather variations [9, 10]. Unlike intermittent renewable energy sources such as solar and wind power, geothermal systems can deliver stable baseload electricity generation 24 hours a day, 7 days a week. Conventional geothermal power plants are based on natural hydrothermal reservoirs but are

often constrained in deployment by geological factors. To overcome these problems, Enhanced Geothermal Systems (EGS) have been developed to exploit thermal energy from deep hot rock formations by artificially stimulating reservoirs and engineering fluid circulation paths [11, 12]. Recent developments in drilling technologies, reservoir stimulation techniques, and heat extraction methods have significantly improved the applicability of EGS for sustainable electricity generation [13]. Various investigations have been performed to study the performance of geothermal power plants with steam turbines and flash cycles and Organic Rankine Cycles (ORCs) for low and medium temperature geothermal resources [14]. These technologies have shown encouraging electrical conversion efficiencies, but a significant fraction of the available thermal energy is unused and is typically rejected as waste heat, thus decreasing the overall utilization efficiency of geothermal resources [15]. Thus, coupling geothermal power generation with other energy conversion processes becomes an attractive approach to improve the overall system performance.

Hydrogen is seen more and more as a key energy carrier for the future low-carbon energy systems, as it can be produced from renewable energy sources and used without direct carbon emissions [16]. Among the available technologies for hydrogen production, alkaline water electrolysis is still one of the most mature and commercially established methods due to its relatively low capital cost, simple construction, long operational lifetime, and high reliability [17]. Recent studies have been directed towards the improvement of electrolyzer performance by optimizing electrode materials, cell configurations, electrolyte composition, and operating parameters. Nickel-based electrodes have been shown to possess better catalytic activity and corrosion resistance than conventional metallic electrodes, which leads to increased hydrogen evolution rates and improved energy efficiency [18]. Similarly, the electrolyte concentration is a significant factor that affects the ionic conductivity, electrical resistance, and the overall system performance. Despite major advances in electrolysis technology, there are relatively few studies on direct integration of alkaline electrolyzers with geothermal-based electricity generation systems, especially for decentralized and small-scale renewable energy applications [19].

Freshwater shortage is one of the most pressing global challenges, especially in arid and semi-arid areas with limited conventional water resources. Solar distillation is regarded as one of the simplest and environmentally sustainable technologies for desalination, due to reliance on renewable solar energy and its minimal operational complexity [20]. Nevertheless, conventional solar stills are often limited in practical applications because of their relatively low freshwater productivity. To overcome this limitation, many researchers have studied performance-enhancing techniques such as thermal energy storage systems, phase change materials, solar collectors, nanofluids, and external heating sources. These methods typically increase the temperature of basin water and increase evaporation rates and therefore increase the production of freshwater [21]. More recently, waste heat recovery has been a very effective strategy to improve desalination performance with no additional fuel consumption. In several studies [22, 23], it has been shown that the use of low-grade waste heat from industrial processes and power generation systems significantly increases the productivity of solar stills and also increases the overall energy utilization efficiency.

Multi-generation systems are of great interest in research as an effective way to optimize energy utilization by producing a number of valuable outputs from a single energy source simultaneously [24]. Such systems often combine electricity generation, heating, cooling, hydrogen production, and freshwater generation into one energy conversion system. The concept of thermal cascading is well known as a promising manner to increase the total efficiency by using sequentially energy streams at different levels of temperature [25]. Many theoretical and thermodynamic studies have shown that multi-generation systems based on renewable energy sources can achieve much higher overall efficiencies than stand-alone energy conversion technologies [26]. In particular, geothermal energy is a strong candidate for supporting integrated energy systems, due to its continuous operation and high thermal availability [27]. However, most of the published investigations are mainly based on thermodynamic analysis, simulation studies, optimization approaches, or techno-economic assessments. Experimental demonstrations of geothermal-driven multi-generation systems for simultaneous production of electricity, hydrogen, and freshwater are still relatively few [28].

Furthermore, experimental validation of practical applications of thermal cascading concepts based on electricity generation, hydrogen production through electrolysis, and desalination improvement through the recovery of turbine exhaust heat has been limited. Therefore, more experimental studies are needed to assess the technical feasibility, performance characteristics, and thermal integration benefits of such systems under realistic operating conditions.

From the literature survey, most of the previous studies have focused on geothermal electricity generation, alkaline water electrolysis, and solar desalination as separate technologies. While several theoretical multi-generation concepts are proposed, comprehensive experimental investigations incorporating these three processes in a single geothermal-driven platform are scarce. Moreover, little attention has been paid to the use of turbine exhaust heat to enhance desalination and to the combined experimental-numerical validation of the system performance. In this context, the present work presents and experimentally investigates an integrated geothermal multi-generation system for simultaneous electricity, HHO, and freshwater desalination production. The proposed system is based on a thermal cascading configuration of a micro steam turbine-generator unit, an alkaline water electrolyzer, and a waste-heat assisted solar still. In addition, three-dimensional CFD simulations are performed to study the heat transfer and fluid flow behavior and to validate the experimental observations, thus providing a comprehensive assessment of the proposed integrated renewable energy-water production system.

1.2 Research gap

Despite the growing interest in the use of geothermal energy and multi-generation technologies, there are still several important research challenges that need to be addressed. Most of the current geothermal studies are based on electricity generation as a single output, which causes considerable thermal energy loss through waste-heat rejection. Second, the production of HHO and desalination systems is usually studied separately, which limits the total utilization of available renewable energy resources. Third, there are few experimental studies on the integration of geothermal power generation, alkaline water electrolysis, and freshwater production in one platform. Moreover, the effective recovery and utilization of the heat of the low-pressure turbine exhaust for desalination enhancement has not been well studied under actual operating conditions. There is a significant gap in knowledge in experimentally validated studies that combine thermal cascading, HHO production, and desalination into an integrated geothermal framework. Such limitations need to be overcome for the overall efficiency of energy utilization to be increased and the economy of renewable resource systems to be improved.

1.3 Objectives of the Current Study

The main objective of this work is to design and experimentally evaluate an integrated geothermal multi-generation system able to simultaneously produce electricity, HHO, and fresh water. The particular objectives are to design and construct a laboratory-scale geothermal energy prototype with power generation, HHO production, and desalination subsystems. The present work aims to study the performance of a geothermal thermal energy-driven micro steam turbine-generator unit. To assess the HHO production performance of alkaline water electrolysis based on different electrode materials, cell configurations, and electrolyte concentrations.

1.4 Contributions of this Study and Novelty

This work is novel in that it experimentally demonstrates and fully evaluates an integrated geothermal-driven multi-generation system that generates electricity, produces HHO, and desalinates freshwater, all in one thermally coupled platform. The main contributions of this research can be summarized as follows:

- Development of a prototype of a closed-loop geothermal multi-generation system with a micro steam turbine, alkaline electrolyser, and waste heat-assisted solar still.
- Experimental investigation of the HHO production performance with different electrolyzer configurations, electrode materials, and electrolyte concentrations.
- Integration of a turbine exhaust heat with a desalination subsystem to enhance the freshwater productivity by thermal energy cascading.
- Assessment of the quality of the produced freshwater.
- CFD-based numerical investigation of temperature distribution, heat transfer characteristics, and fluid flow behavior with experimental validation.
-

2. THE PROPOSED SYSTEM DESCRIPTION AND EXPERIMENTAL METHOD

2.1 System Description

An integrated multi-generation system based on geothermal was developed and experimentally evaluated for simultaneous production of electrical power, HHO (hydrogen and oxygen) gas, and desalinated freshwater. The proposed configuration adopts a thermal cascading strategy to enhance the use of geothermal energy by sequentially

converting the available thermal energy into multiple useful products. The system developed consists of four thermally integrated subsystems:

- A steam generator as a simulator of geothermal heat sources.
- A micro steam turbine with a DC electrical generator.
- An alkaline water electrolyser for HHO production.
- A solar still with heat recovery from the turbine exhaust.

The operating principle of the system is shown schematically as shown in **Figure 1**. First, water is heated in the geothermal boiler until superheated steam is produced. The steam is fed to a single-stage impulse micro-steam turbine for conversion of thermal to mechanical power. The turbine shaft is directly connected to a DC generator to generate electricity. The produced electrical power is then supplied to the alkaline electrolyzer for HHO production. Simultaneously, the low-pressure exhaust steam from the turbine is used as a secondary heat source by a submerged copper heat exchanger located inside the basin of the solar still. This recovered thermal energy increases the temperature of the basin water, increasing the evaporation rate and hence the fresh water productivity. The condensed working fluid is fed back to the boiler by a circulation pump. This completes a closed - loop geothermal cycle. This integrated configuration reduces thermal losses and improves the overall utilization of resources compared to traditional separate systems for electricity generation, HHO production, and desalination. **Figure 2** shows photographs of the developed experimental setup and its main components.

2.2 The System Components

2.2.1 Unit for Geothermal Heat Source and Steam Generation

The thermal behavior of an Enhanced Geothermal System (EGS) was simulated by a laboratory-scale boiler. The boiler produced superheated steam at specified operating conditions and fed it continuously to the turbine inlet. Because of its high thermal conductivity and good corrosion resistance, the steam transport and heat recovery sections were constructed from copper tubing.

2.2.2 Micro Steam Turbine & Electrical Generator

The power generation subsystem consisted of a single-stage impulse micro-steam turbine connected directly to a 12 V DC generator. The turbine rotor was 60 mm in diameter and had twelve stainless steel blades to withstand high steam temperatures and velocities. During operation, the process of steam expansion transformed thermal energy into rotational mechanical power, which was then converted into electrical energy by the generator. The experimental measurements showed an average electrical power output of about 31 W, sufficient to continuously operate the electrolyzer.

2.2.3 Alkaline water electrolysis

HHO production was carried out using a custom-built alkaline water electrolyzer powered directly by the electricity produced by the turbine-generator unit. The electrolyzer is composed of nickel-plated SS316 electrodes with an effective active area of 255 cm2. The electrolyte was a potassium hydroxide (KOH) solution with high ionic conductivity and good electrochemical properties. Different electrode arrangements and cell configurations were tested to determine the best operating conditions for HHO production. The electrolyzer body was composed of transparent acrylic plates that were sealed together with rubber O-rings to prevent electrolyte leakage and loss of gas.

2.2.4 Solar Still Powered by Waste Heat

The desalination subsystem was composed of a single-basin solar still with a basin area of 0.25m2. The basin was made of galvanized steel and wrapped in a thermally insulated housing to minimize the heat losses to the environment. A transparent glass cover with an inclination angle of 30° and a thickness of 4 mm was installed to allow the condensation of vapor and the collection of fresh water. A submerged copper heat exchanger was placed in the saline-water basin to recover thermal energy from the turbine exhaust steam. The recovered waste heat remarkably enhanced the thermal energy delivered to the desalination unit, which resulted in a significant enhancement of the evaporation and condensation processes. Experimental results indicated that the freshwater productivity increased to 8.6 L/day with the assistance of waste heat recovery.

2.3 Experimental procedure

An experimental investigation was carried out in the Mechanical Engineering Department, Faculty of Engineering, Suez Canal University, Ismailia, Egypt. Before each experimental run, the boiler was filled with water and heated to the desired steam temperature and pressure. The produced steam was then transferred to the turbine, where the electrical power was generated and directly fed into the alkaline electrolyzer. Simultaneously, the turbine exhaust steam was sent to the immersed heat exchanger placed in the basin of the solar still. The recovered thermal energy increased the saline water temperature and improved the desalination process. During each experiment, the following parameters were continuously monitored and recorded:

- Steam pressure, temperature.
- Turbine speed.
- Output voltage and current.
- HHO production rate
- Water temperature in the basin.
- Freshwater productivity.
- Ambient conditions

HHO production was measured by the volumetric water-displacement method, and freshwater yield was quantified with a calibrated graduated cylinder. Water quality was analyzed before and after desalination to assess the efficiency of the treatment process. Each experimental condition was repeated three times to ensure repeatability and reliability, and the values reported are the average of the measured results.

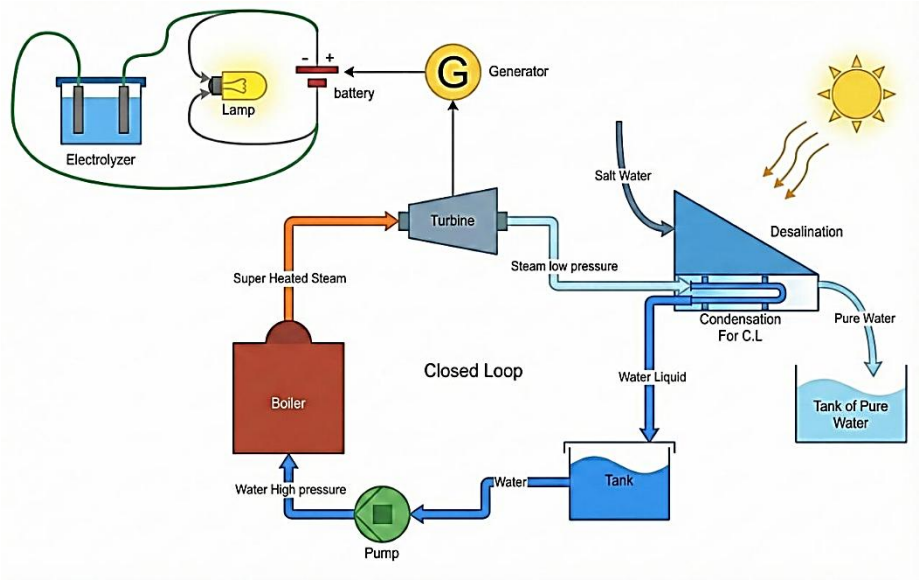

Figure 1. Schematic diagram for the experimental setup

(a) Electrode plate

(b) Electrolyser

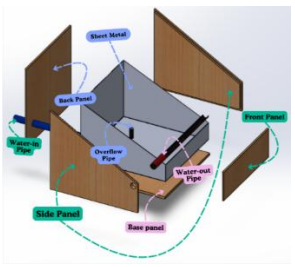

(c) Solar still components

(d) Battery

(e) Thermocouple

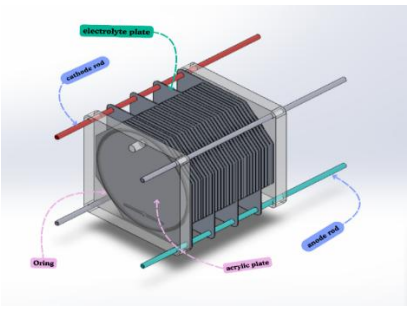

(f) Electrolyser components

Figure 2. Photo of the system setup with different components

2.4 Analysis of Uncertainty

The procedure outlined by [29] was used to compute measurement uncertainties. The uncertainty U in the measured parameters is provided by the following if the instrument accuracy is ±a:

$$\text{Standard Uncertaintiy (U)} = \frac{\text{Accuracy (a)}}{\sqrt{3}} \quad (1)$$

The root-sum-square method was used to estimate the combined uncertainty (δ) for the derived parameters, such as efficiency:

$$\delta = \sqrt{\left(\frac{\partial F}{\partial x}\right)^2 \delta_x^2 + \left(\frac{\partial F}{\partial y}\right)^2 \delta_y^2} \quad (2)$$

Where the measured variables x and y uncertainties are denoted by δx and δy, respectively. The partial derivatives of the targeted parameter F with respect to x and y are ∂F/∂x and ∂F/∂y. Instrumentation, accuracy, and total uncertainties for the measured parameters are presented as shown in **Table 1**. From this table, it can be seen that all values fall within the permissible range, which indicates the overall reliability of the thermal performance evaluation.

Table 1. Instrumentation, accuracy, and total uncertainties for the measured parameters.

No.	Parameter	Instrument	Accuracy, a	Uncertainty, U
1	Solar radiation, W/m^2	Solar wattmeter	± 1.0	0.58
2	Temperature, ºC	K-type thermocouple	± 0.01	0.0058
3	Water yield, ml	Flask	± 10	5.8
4	Time, s	Stopwatch	±1 s	0.58

3. MATHEMATICAL MODEL AND NUMERICAL APPROACH

A combined experimental and numerical approach was used to study an integrated geothermal multi-generation system in order to estimate its thermal, hydrodynamic, and electrochemical performance. The system is composed of a geothermal steam generator, a micro-steam turbine coupled to a DC generator, an alkaline water electrolyzer for hydrogen production, and a solar still desalination unit that uses the solar energy and the heat from the turbine exhaust. The heat transfer characteristics, steam flow behaviour, pressure distribution, and temperature fields of the overall turbine, heat recovery unit, and desalination chamber are analysed by means of three-dimensional Computational Fluid Dynamics (CFD) simulations by using ANSYS Fluent. Conservation equations under steady-state conditions were solved by the finite volume method. The numerical predictions were confirmed by experimental measurements on the prototype system.

3.1 Governing Equations

The fluid flow and heat transfer phenomena inside the system are governed by the conservation laws of mass, momentum, and energy. The conservation of mass is expressed as [30, 31]:

$$(\nabla . V) = 0 \quad (3)$$

Where V is the velocity vector (m/s). This equation states that the mass entering a control volume is equal to the mass leaving the control volume.

The transport of momentum in the fluid domain is governed by the Navier-Stokes equation:

$$\rho(V.\nabla V) = -\nabla P + \nabla.(\mu \nabla V) + \rho g \quad (4)$$

Where P is the pressure, μ is the dynamic viscosity, and g is the gravitational acceleration.

The energy conservation equation can be written as:

$$\rho C_P(V.\nabla T) = \nabla.(k\nabla T) + Sh \quad (5)$$

Where C_P is the specific heat capacity, k is the thermal conductivity, and Sh represents the volumetric heat source term.

3.2 Turbulence Model

The steam flow in the turbine nozzle, rotor passages, and heat recovery sections is typically turbulent. The standard k–ε turbulence model was therefore used, due to its robustness and efficiency in engineering calculations. The standard k-ε turbulence model was employed to describe the turbulent steam flow inside the turbine and heat recovery sections.

The transport equation for turbulent kinetic energy is:

$$\rho(V.\nabla k) = \nabla.[(\mu + \mu t/\sigma k)\nabla k] + Gk - \rho\varepsilon \quad (6)$$

Where: k is the turbulent kinetic energy (m^2/s^2), μ_t is the turbulent viscosity, σ_k is the turbulent Prandtl number for k, G_k, represents turbulence production due to velocity gradients, and ε is the turbulence dissipation rate.

The transport equation for turbulence dissipation rate is:

$$\rho(V.\nabla\varepsilon) = \nabla.[(\mu + \mu t/\sigma\varepsilon)\nabla\varepsilon] + C_1\varepsilon(\varepsilon/k)Gk - C_2\varepsilon\rho(\varepsilon^2/k) \quad (7)$$

Where: C_1 =1.44, C_2 =1.92, σ_ε=1.3.

3.3 Thermal Energy and Steam Production Analysis

The total thermal energy required for steam generation consists of sensible heating and latent heat of vaporization:

$$Q_{th} = m_w C_P(T_s - T_i) + m_w h_{fg} \quad (8)$$

Where: Q_{th} is the total thermal energy supplied (W), m_w is the water mass flow rate (kg/s), T_i is the inlet water temperature (°C), T_s is the saturation temperature (°C), h_{fg} is the latent heat of vaporization (kJ/kg).

The mass flow rate is calculated from:

$$\dot{m}_s = Q_{th}/(h_g - h_f) \quad (9)$$

Where h_g and h_f are the specific enthalpies of saturated steam and saturated liquid water, respectively.

3.4 Micro-Steam Turbine Performance

The theoretical steam velocity at the nozzle exit is obtained from the steady-flow equation [32, 33]:

$$V_1 = \sqrt{[2\eta(h_{in} - h_{out})]} \quad (10)$$

Where: V_1 is the nozzle exit velocity (m/s),η_n is the nozzle efficiency, h_{in} and h_{out} are the inlet and outlet steam enthalpies (kJ/kg).

The mechanical power produced by the turbine is calculated using Euler's turbine equation:

$$P_t = \dot{m}_s(U_1V_{w1} - U_2V_{w2}) \quad (11)$$

Where U represents blade velocity and V_w represents the whirl component of steam velocity.

The turbine efficiency is determined from:

$$\eta_t = \frac{P_t}{[\dot{m}_s(h_{in} - h_{out})]} \times 100 \quad (12)$$

3.5 Electrical Power Generation

The electrical power generated by the DC generator that converts mechanical energy into electrical energy is calculated as:

$$P_e = VI \quad (13)$$

Where V is the output voltage and I is the output current.

The generator efficiency is determined from:

$$\eta_g = \frac{P_e}{P_t} \times 100 \quad (14)$$

3.6 Alkaline Water Electrolyzer Model

HHO production is evaluated according to Faraday's law of electrolysis [7, 19]:

$$\dot{m}_{H_2} = \frac{IM_{H_2}}{nF} \quad (15)$$

Where M_{H2} is the molecular weight of HHO, n is the number of electrons transferred, and F is Faraday's constant. The volumetric HHO production rate is obtained from:

$$V_{H_2} = \frac{\dot{m}_{H_2}}{\rho_{H_2}} \quad (16)$$

Where ρ_{H2} is the HHO density.

The electrolyzer efficiency is expressed as:

$$\eta_{el} = \frac{\dot{m}_{H_2} \times LHV_{H_2}}{P_e} \times 100 \quad (17)$$

Where LHV_{H2} is the lower heating value of HHO.

3.7 Solar Still Performance Analysis

The desalination subsystem utilizes direct solar energy and waste heat recovered from the turbine exhaust steam. The solar thermal energy absorbed by the basin water is [34, 35]:

$$Q_s = IA\alpha \quad (18)$$

Where I is the solar irradiance and A is the basin area. The thermal energy recovered from turbine exhaust steam is calculated as:

$$Q_{rec} = \dot{m}_s(h_{in} - h_{out}) \quad (19)$$

The total thermal energy supplied to the desalination chamber is:

$$Q_{total} = Q_s + Q_{rec} \quad (20)$$

The evaporation rate of saline water is determined from:

$$\dot{m}_{ev} = \frac{Q_{total}}{h_{fg}} \quad (21)$$

The thermal efficiency of the solar still is calculated as:

$$\eta_{ss} = \left(\frac{\dot{m}_d h_{fg}}{Q_{total}}\right) \times 100 \quad (22)$$

Where $\dot{m}_d$ is the freshwater

3.8 Mesh Independence Study

A mesh independence study is performed to ensure that the numerical results are not influenced by the mesh density. The computational domain, including the steam turbine, heat exchanger, and solar still, was created with four different mesh sizes. Since the desalination performance is directly affected by the water temperature, the average basin water temperature was selected as the monitoring parameter as shown in **Table 2**.

Table 2. Mesh independence study

Mesh Level	Number of Cells	Basin Water Temperature (°C)	Difference (%)
Coarse	245,000	68.2	—
Medium	487,000	70.1	2.79
Fine	742,000	70.8	0.99
Very Fine	1,025,000	71.0	0.28

It can be seen that the difference between the fine and very fine mesh was less than 1%, which means the numerical solution became insensitive to the mesh density. Therefore, the mesh with approximately 742,000 cells was selected for all subsequent simulations, as it offered a suitable balance between computational accuracy and computational time.

3.9 Overall System Energy Efficiency

The overall energy efficiency of the proposed geothermal multi-generation system was evaluated in terms of the useful outputs of electricity generation, HHO production, and freshwater production with respect to the thermal energy supplied by the geothermal heat source. The overall efficiency is given as:

$$\eta_{overall} = \frac{P_e + \dot{m}_{H_2} \times LHV_{H_2} + \dot{m}_d h_{fg}}{Q_{geothermal}} \times 100 \quad (23)$$

where P_e is the net electrical power output from the turbine–generator unit, $\dot{m}_{H_2}$ is the HHO production rate, LHV_{H_2} is the lower heating value of HHO representing its chemical energy content, $\dot{m}_d$ is the freshwater production rate, h_{fg} is the latent heat of vaporization of water, and $Q_{geothermal}$ is the thermal energy supplied by the geothermal source.

4. RESULTS AND DISCUSSIONS

4.1 Performance of the Geothermal Power Generation System

The feasibility of the power generation subsystem, geothermal, was evaluated to convert the thermal energy into useful electrical power to drive the HHO production unit. The developed system employed a laboratory-scale steam turbine directly coupled to a DC generator, which represents the first stage of the thermal cascading process. In operation, the superheated steam formed in the geothermal boiler expanded through the turbine blades, converting thermal energy to mechanical power. The turbine shaft was directly coupled to a DC generator. The rotational energy was converted into electrical energy, without intermediate transmission components. This configuration reduced mechanical losses and enhanced the overall reliability of the system. The experimental results show the stable operation of the turbine during the testing period. The electrical output obtained was found to be only slightly sensitive to changes in steam temperature and pressure. The average electrical power produced by the turbine-generator unit was about 31 W, sufficient to operate the alkaline electrolyzer for HHO production continuously. The power output obtained confirms the feasibility of using low-scale geothermal energy systems for decentralized electricity generation. The produced power is relatively small compared to commercial geothermal plants, but it is sufficient to serve the energy demand of the HHO production subsystem and shows the effectiveness of the proposed integrated configuration. The developed multi-generation platform also has the advantage of thermal cascading for the successful operation of the turbine-generator sub-system. Instead of venting the turbine exhaust steam directly to the environment, residual thermal energy was recovered by means of a heat exchanger and used to improve the desalination process. Therefore, the generated electrical energy and the recovered thermal energy both enhanced the overall system utilization efficiency. The consistent production of electrical power over the experimental period indicated a dependable renewable energy source for HHO production and the feasibility of integrating geothermal power generation with electrolysis and desalination technologies on a single sustainable platform.

4.2 Assessment of HHO Production

Figure 3 displays the mean voltage and time required to produce 1 L of HHO gas with stainless-steel electrodes at 10% KOH electrolyte concentration for both electrolyzer designs. For the two-cell configuration, the average operating voltage was around 7.61 V, and the time to produce 1 L of HHO was around 25.31 min. More cells (4) yield a higher operating voltage of approximately 9.44 V. However, the required production time decreased significantly to almost 21.01 min. The larger active electrochemical surface area available in the four-cell arrangement, which improved the ion transport and increased the rate of HHO generation, was attributed to this behavior. The reduction in production time indicates a positive effect of increasing the number of electrolysis cells on the total HHO production rate. The additional cells increased the amount of reaction sites, which resulted in improved electrochemical performance and better utilization of the electrical power generated by the geothermal-driven turbine-generator system. **Figure 4**. Variation of power consumption and electrolyzer efficiency for both cell configurations. The two-cell electrolyzer consumed approximately 0.732 Wh/L, and the efficiency was nearly 68.3%. The four-cell configuration, however, consumed a slightly higher amount of power, about 0.760 kW, but showed a higher efficiency of almost 79%. This increased efficiency indicates that the additional cells reduced the losses due to internal resistance and increased the efficiency of the electrochemical conversion of electrical energy into chemical energy stored in HHO gas. These results confirm that the HHO production performance can be improved by increasing the number of electrolysis cells while keeping the energy consumption at an acceptable level. The obtained efficiencies are in agreement with those reported for alkaline water electrolysis systems working with KOH electrolytes, showing that the developed geothermal-powered electrolyzer is capable of producing HHO efficiently using renewable energy.

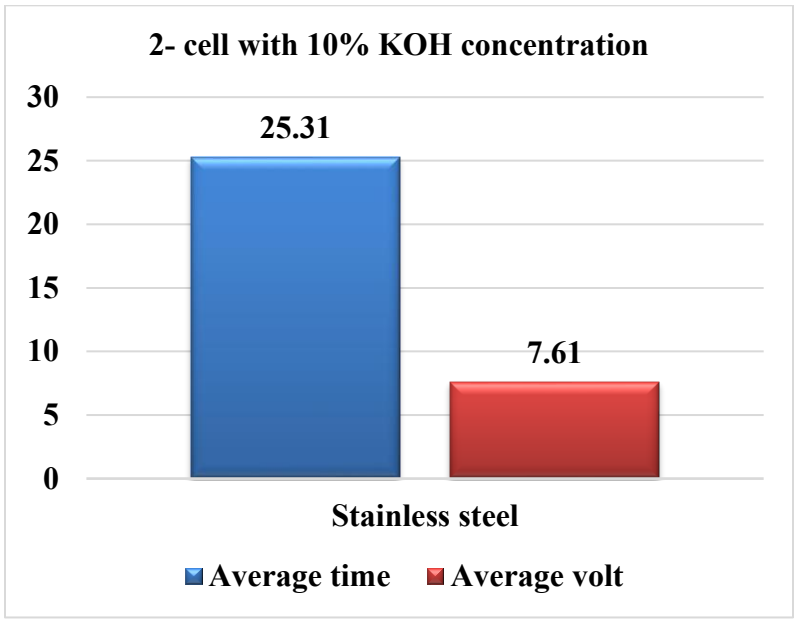

(a)

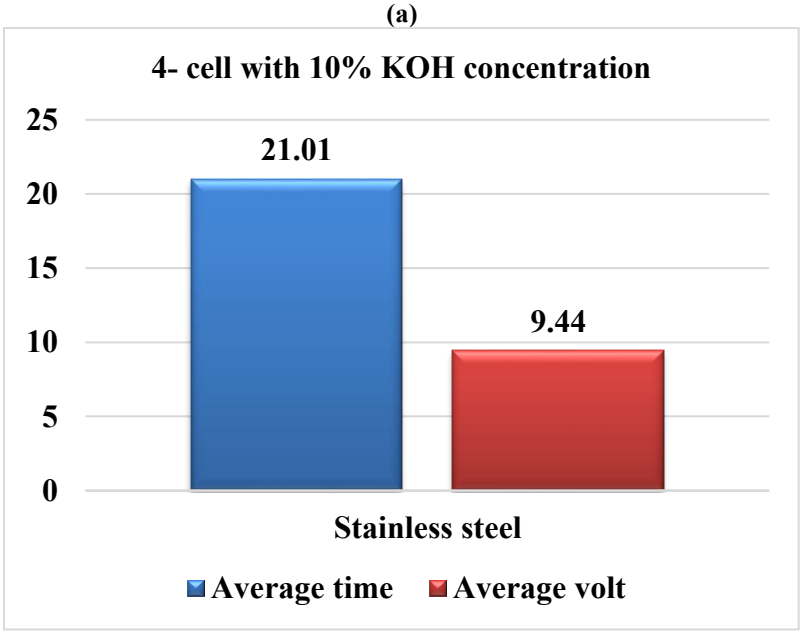

(b)

Figure 3. Variation of average voltage and time required to produce 1 Liter of HHO using 2 and 4 cells for Stainless steel

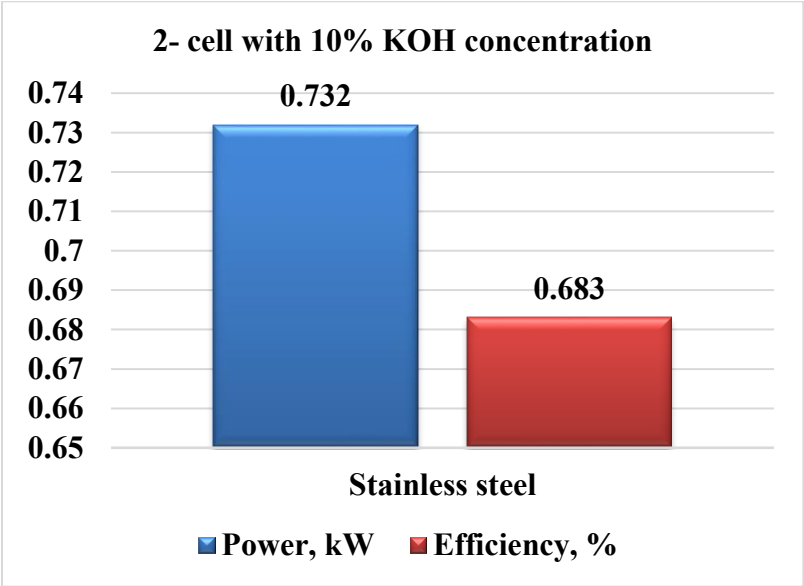

(a)

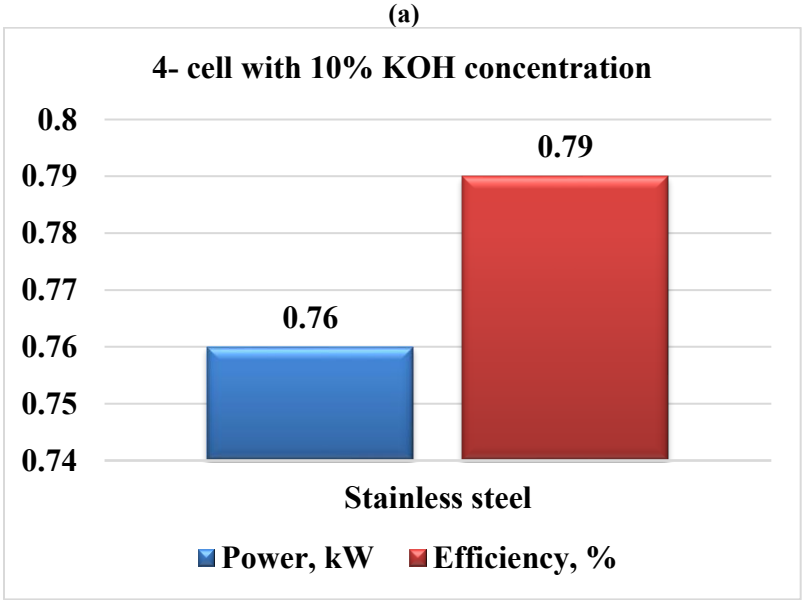

(b)

Figure 4. Variation of average power and efficiency required to produce 1 Liter of HHO using 2 and 4 cells for Stainless steel

4.3 Solar Still Performance

Figure 5, Change of solar radiation intensity during the experimental day. As expected, the solar irradiance increased gradually in the morning hours due to the increasing solar elevation angle and reached its maximum value around solar noon. The radiation intensity then gradually decreased in the afternoon period. The solar radiation was more than 1000 W/m2 during the midday hours, which offered good conditions for the evaporation process inside the solar still. The observed radiation profile is typical of such climatic conditions (clear sky) and is the main source of energy driving the evaporation process in the desalination unit. The accumulated daily freshwater productivity is shown in **Figure 6**. The yield of fresh water increased continuously with time of operation due to the continuous processes of evaporation and condensation. The productivity in the early morning period was relatively low due to the still-increasing basin water temperature. The increased solar radiation and more thermal energy from the turbine exhaust heat recovery system led to a significantly higher evaporation rate. Integration of waste heat recovery with solar still

enhanced thermal utilization and significantly enhanced freshwater production. The experiments showed that using turbine exhaust heat in the conventional operation increased the fresh water productivity to 8.6 L/day. This remarkable increase confirms the effectiveness of thermal cascading and waste heat recovery to improve the desalination performance. The additional thermal energy provided by the turbine exhaust increased the temperature of the basin water, enhanced the evaporation, and helped to increase the condensation rates on the glass cover.

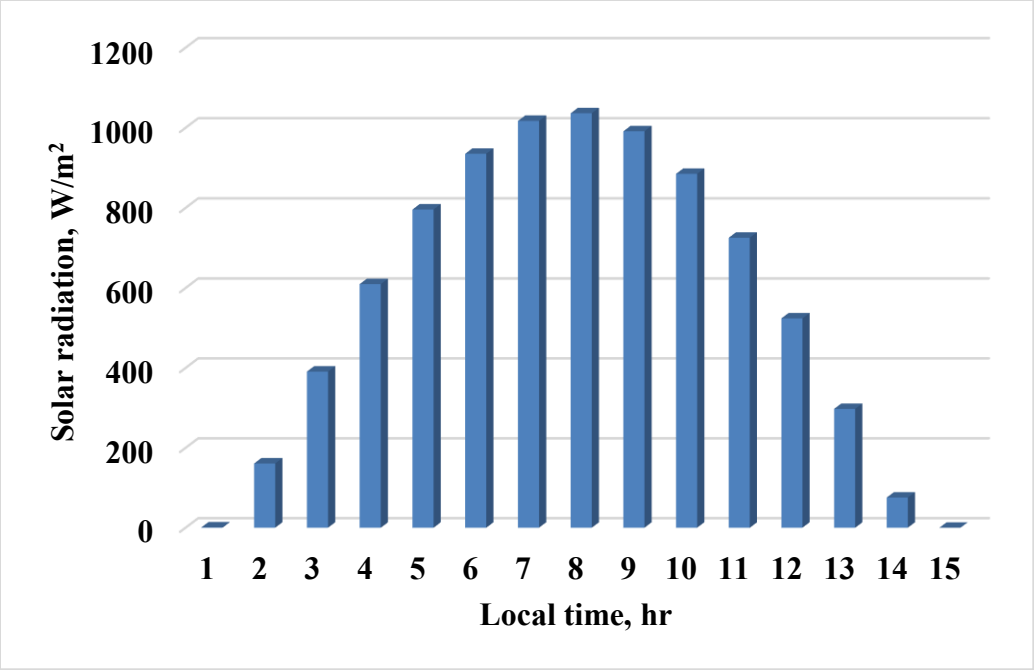

Figure 5. Variation of solar radiation with local time

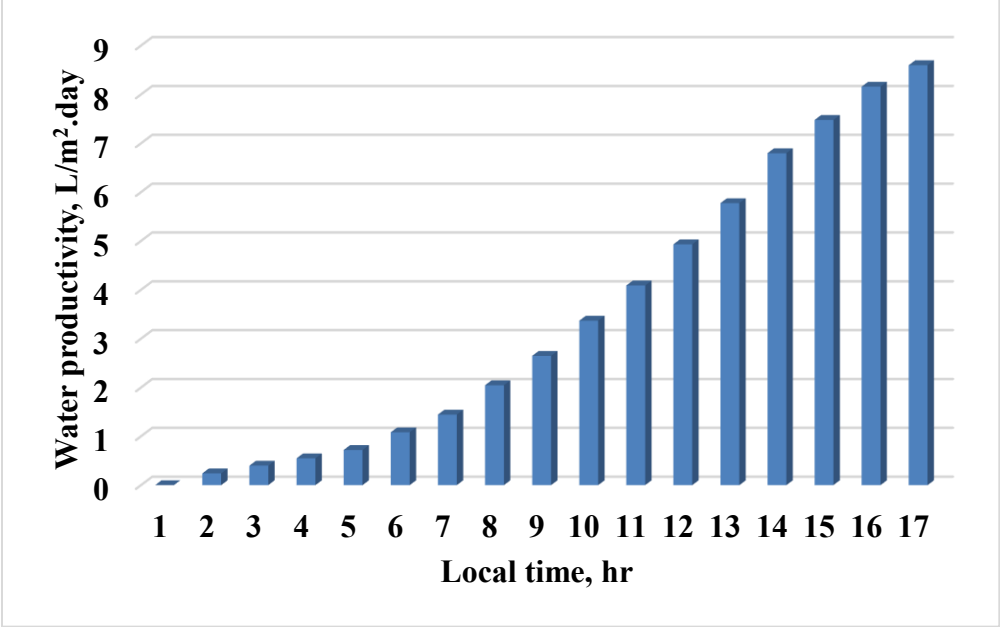

Figure 6. Variation of accumulated productivity with local time for the solar still

4.4 Results of CFD Modelling

Figure 7 shows the temperature contour from the CFD simulation of the submerged heat exchanger. The results show that the heat is effectively transferred from the turbine exhaust steam to the ambient saline water. Higher temperatures were found in the vicinity of the inlet section of the heat exchanger, while a gradual decrement of temperature was observed in the direction of flow due to heat extraction by the basin water. The temperature distribution corroborates the successful recovery of waste thermal energy and displays the ability of the heat exchanger to provide a continuous supplementary heat source to the desalination process. **Figure 8** shows the temperature contour in the steam turbine. The simulation results show that the steam temperature decreases from the inlet of the turbine to the outlet as the thermal energy is converted into mechanical work. The highest temperatures are located in the region of steam admission, and the lowest temperatures are in the exhaust section. The predicted temperature gradients are consistent with the expected thermodynamic expansion process occurring inside the turbine, and they confirm the efficiency of the turbine in extracting useful work from the geothermal steam. The temperature distribution within the solar still obtained from CFD simulations is presented in **Figure 9**. The contour shows the higher temperatures near the region of the submerged heat exchanger and the basin water. The temperature difference between the warm water surface and the relatively cooler glass cover makes the conditions suitable for evaporation and condensation. Numerical results demonstrate that the recovered turbine exhaust heat significantly enhances the basin water temperature and the thermal conditions for freshwater production. The observations are in good agreement with the increase in productivity measured experimentally.

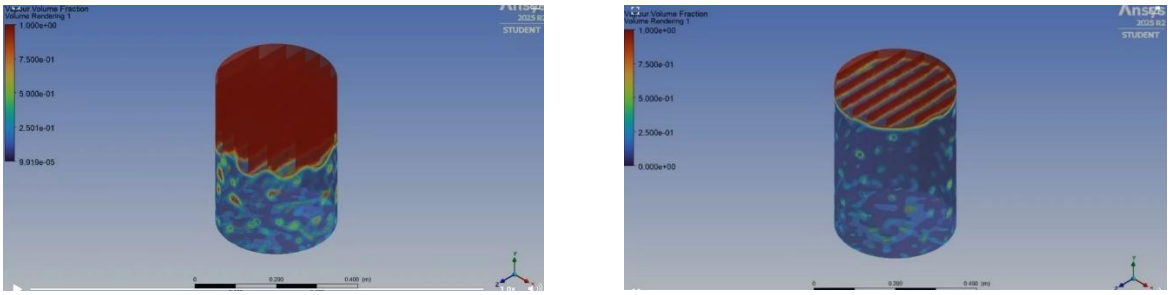

Figure 7. ANSYS Fluent thermal contour for heat exchanger here

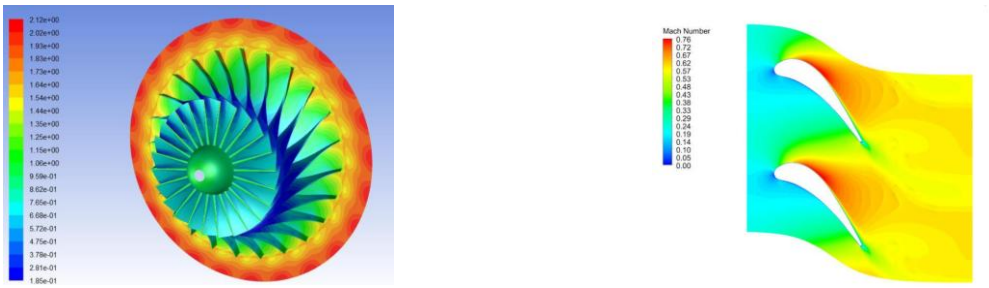

Figure 8. ANSYS Fluent thermal contour for steam turbine

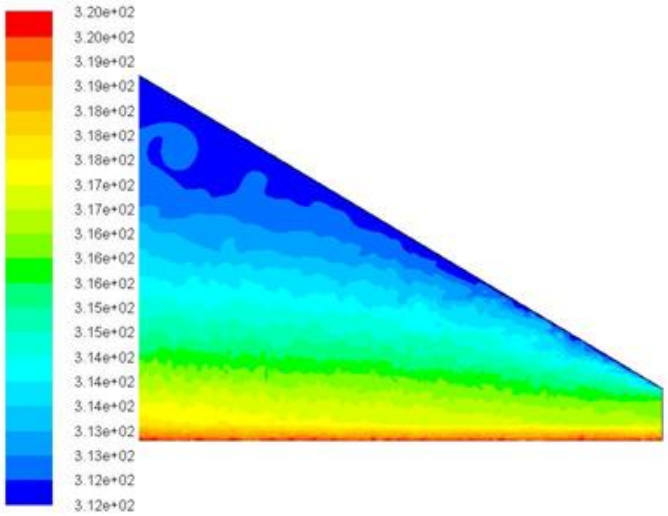

Figure 9. Solar still temperature contour

4.5 Water Quality Analysis

Table 3 delineates the water quality features before and after desalination. In terms of total dissolved solids (TDS) concentration, there was a dramatic decrease from approximately 1000 - 4000 ppm in the feed water to just 27 ppm in the produced freshwater. In addition, the pH value of the distilled water was within the permissible drinking-water range recommended by the World Health Organization (WHO). The results obtained showed the high efficiency of the developed desalination unit in removing the dissolved salts and producing high-quality freshwater suitable for domestic and drinking applications. The obtained water quality confirms that the combination of geothermal energy and waste heat recovery can provide energy and clean water simultaneously on an integrated, sustainable platform.

Table 3. Results of water quality analysis.

Parameter	Input brackish water	Output from the solar still	WHO standard [36]
Total dissolved solids (TDS), ppm	1000 – 4000	76	≤ 500
pH	6.5–8.5	6.6	≤ 6.5–8.5

4.6 CFD Model Validation

The validation of the numerical model was carried out by comparing the CFD predictions from ANSYS Fluent with the experimental measurements at the same operating conditions. The comparison was made for the basic thermal parameters such as the temperature at the turbine outlet, the temperature at the heat exchanger outlet, and the temperature of the basin water of the solar still as shown in **Table 4**.

Table 4. Comparison between experimental and CFD results.

Parameter	Experimental	CFD Prediction	Error (%)
Turbine outlet temperature (°C)	112.5	119.3	6.0
Heat exchanger outlet temperature (°C)	84.7	89.1	5.2
Basin water temperature (°C)	69.4	72.8	4.9
Glass cover temperature (°C)	48.6	50.7	4.3

The maximum deviation between numerical and experimental results was approximately 6%, while the average deviation was about 5.1%. These results demonstrate good agreement between the CFD simulations and the experimental measurements and confirm the reliability of the developed numerical model for predicting heat transfer and fluid flow characteristics within the integrated geothermal multi-generation system.

4.7 Overall System Energy Efficiency

Based on the experimental measurements, the average electrical power output was 31 W. The four-cell alkaline electrolyzer achieved an efficiency of approximately 79%, corresponding to a HHO energy output of about 24.5 W. The freshwater productivity reached 8.6 liters per day, corresponding to an equivalent thermal output of approximately 248 W. Therefore, the total useful energy output was 303.5 W. Since the thermal input supplied by the geothermal boiler was 1 kW, the overall system efficiency was calculated as 30.35%. The obtained efficiency demonstrates the effectiveness of the thermal cascading concept, where the geothermal energy is sequentially utilized for electricity generation, HHO production, and desalination. The recovery of turbine exhaust heat significantly enhanced the overall utilization of the supplied thermal energy and reduced energy losses compared with conventional stand-alone systems.

5. CONCLUSION

A laboratory scale geothermal based multi-generation system was successfully designed, built and experimentally studied to simultaneously produce electricity, HHO gas and fresh water. The proposed configuration successfully integrated geothermal power generation, alkaline water electrolysis and solar desalination via a thermal cascading approach to maximize energy utilization and minimize thermal losses. On the basis of the experimental and numerical investigations the following conclusions can be drawn:

- The geothermal steam turbine-generator subsystem operated successfully, with an average electrical power output of ~ 31 W, demonstrating the small scale geothermal resources' capability to provide continuous renewable electricity for decentralized applications.

- The electricity generated was sufficient to run the alkaline water electrolyser without interruption. The number of electrolysis cells were increased from two to four, which improved HHO production performance and reduced the time taken to produce HHO gas and increased the electrolyzer efficiency from about 68% to about 79%.

- The recovery of turbine exhaust heat using a submerged heat exchanger to improve the thermal performance of the solar still. The additional thermal energy increased the evaporation rate, and enhanced the freshwater productivity from to 8.6 liter per day, which confirmed the effectiveness of waste heat recovery for desalination enhancement. The water quality analysis indicated that the desalination process was very successful in lowering the total dissolved solids concentration to about 76 parts per million which is well below the recommended levels for drinking water.

- CFD simulations could predict the temperature distributions and heat transfer characteristics in the turbine, heat exchanger and solar still. The numerical results were in good agreement with experimental measurements with deviations less than 7% which confirmed the reliability of the developed numerical model.

- The integrated geothermal multi-generation system proved the practical feasibility of producing renewable electricity, HHO fuel and freshwater at the same time from one energy source. The thermal cascading strategy improved the overall utilization of resource significantly comparing with the conventional stand-alone systems.

Overall, the proposed system provides an efficient and sustainable solution for the joint generation of energy and water and is a promising technology for remote communities, arid regions and off-grid applications with limited access to electricity, clean fuel and freshwater.

FUTURE WORK:

The future work should concentrate on increasing the system capacity, improving the design of the turbine and the electrolyzer, integrating thermal energy storage materials, and performing detailed techno-economic and exergy analyses. Also, the use of real geothermal wells and advanced HHO storage technologies should be investigated to improve the performance and commercial feasibility of the system.

REFERENCE

[1] P. Olasolo, M. C. Juárez, M. P. Morales, S. D'Amico, and I. A. Liarte, "Enhanced geothermal systems (EGS): A review," Renew. Sustain. Energy Rev., vol. 56, pp. 133–144, 2016, doi: 10.1016/j.rser.2015.11.031.

[2] H. Al-Hinai, M. S. Al-Nassri, and B. A. Jubran, "Parametric investigation of a double-effect solar still," Desalination, vol. 146, nos. 1–3, pp. 273–279, 2002, doi: 10.1016/S0011-9164(02)00486-5.

[3] H. Nath, M. N. Mahmood, E. Ofosu, and A. Khanal, "Enhanced geothermal systems: A critical review of recent advancements and future potential for clean energy production," Geoenergy Sci. Eng., vol. 243, Art. no. 213370, 2024, doi: 10.1016/j.geoen.2024.213370.

[4] S.-M. Lu, "A global review of enhanced geothermal system (EGS)," Renew. Sustain. Energy Rev., vol. 81, pp. 2902–2921, 2018, doi: 10.1016/j.rser.2017.06.097.

[5] Y. Feng, J. Zhao, and X. Luo, "Sustainable development of enhanced geothermal systems based on geotechnical research—A review," Earth-Sci. Rev., vol. 199, Art. no. 102955, 2019, doi: 10.1016/j.earscirev.2019.102955.

[6] A. Boretti, "Enhanced geothermal systems: Potential, challenges, and a realistic path to integration in a sustainable energy future," Next Energy, vol. 8, Art. no. 100332, 2025, doi: 10.1016/j.nxener.2025.100332.

[7] K. Zeng and D. Zhang, "Recent progress in alkaline water electrolysis for hydrogen production and applications," Prog. Energy Combust. Sci., vol. 36, no. 3, pp. 307–326, 2010, doi: 10.1016/j.pecs.2009.11.002.

[8] J. Brauns and T. Turek, "Alkaline water electrolysis powered by renewable energy: A review," Processes, vol. 8, no. 2, Art. no. 248, 2020, doi: 10.3390/pr8020248.

[9] K. Ghaffari, J. J. S. de Oliveira, and L. O. Seman, "Exploring geothermal energy as a sustainable source of energy," Sustain. Horizons, vol. 13, Art. no. 100135, 2025, doi: 10.1016/j.horiz.2025.100135.

[10] N. T. Alwan, S. E. Shcheklein, and O. K. Ahmed, "Performance of solar still units and enhancement techniques: A review investigation," Heliyon, vol. 10, no. 18, Art. no. e37693, 2024, doi: 10.1016/j.heliyon.2024.e37693.

[11] S. Ye, G. Feng, J. Xu, X. Zhang, and Y. Zhang, "Artificial intelligence empowering geothermal energy development," Renew. Sustain. Energy Rev., vol. 212, Art. no. 115201, 2025, doi: 10.1016/j.rser.2024.115201.

[12] S. Sebbahi, A. Assila, A. A. Belghiti, S. Laasri, et al., "A comprehensive review of recent advances in alkaline water electrolysis for hydrogen production," Int. J. Hydrogen Energy, vol. 82, pp. 583–599, 2024, doi: 10.1016/j.ijhydene.2024.07.428.

[13] E. Barbier, "Geothermal energy technology and current status: An overview," Renew. Sustain. Energy Rev., vol. 6, nos. 1–2, pp. 3–65, 2002, doi: 10.1016/S1364-0321(02)00002-3.

[14] A. Franco and M. Vaccaro, "Numerical simulation of geothermal reservoirs for the sustainable design of energy plants: A review," Renew. Sustain. Energy Rev., vol. 30, pp. 987–1002, 2014, doi: 10.1016/j.rser.2013.11.041.

[15] R. DiPippo, Geothermal Power Plants: Principles, Applications, Case Studies and Environmental Impact, 4th ed. Amsterdam, The Netherlands: Elsevier, 2016.

[16] M. Ball and M. Wietschel, "The future of hydrogen—Opportunities and challenges," Int. J. Hydrogen Energy, vol. 34, no. 2, pp. 615–627, 2009, doi: 10.1016/j.ijhydene.2008.11.014.

[17] M. Muthiah, M. Elnashar, W. Afzal, and H. Tan, "Safety assessment of hydrogen production using alkaline water electrolysis," Int. J. Hydrogen Energy, vol. 84, pp. 803–821, 2024, doi: 10.1016/j.ijhydene.2024.08.237.

[18] M. Carmo, D. L. Fritz, J. Mergel, and D. Stolten, "A comprehensive review on PEM water electrolysis," Int. J. Hydrogen Energy, vol. 38, no. 12, pp. 4901–4934, 2013, doi: 10.1016/j.ijhydene.2013.01.151.

[19] A. Ursúa, L. M. Gandía, and P. Sanchis, "Hydrogen production from water electrolysis: Current status and future trends," Proc. IEEE, vol. 100, no. 2, pp. 410–426, 2012, doi: 10.1109/JPROC.2011.2156750.

[20] A. E. Kabeel, M. Abdelgaied, and G. M. Mahmoud, "Performance evaluation of continuous solar still water desalination system," Journal of Thermal Analysis and Calorimetry, vol. 144, no. 6, pp. 907–916, 2021, doi: 10.1007/s10973-020-09547-5.

[21] A. E. Kabeel, Z. M. Omara, and F. A. Essa, "Enhancement of pyramid-shaped solar stills performance using a high thermal conductivity absorber plate and cooling the glass cover," Desalination, vol. 281, pp. 400–404, 2011, doi: 10.1016/j.desal.2011.08.018.

[22] A. Fathy, H. Rezk, and A. G. Olabi, "A novel method for optimizing the size of a hybrid solar-wind-battery energy system," Renew. Sustain. Energy Rev., vol. 82, pp. 343–355, 2018, doi: 10.1016/j.rser.2017.09.072.

[23] M. Sharshir, G. Peng, N. Yang, M. O. A. Ali, and A. H. Elsheikh, "A study on heat and mass transfer analysis of solar distillation system," Energy Convers. Manage., vol. 133, pp. 173–183, 2017, doi: 10.1016/j.enconman.2016.11.044.

[24] M. A. Rosen and I. Dincer, "On hydrogen and hydrogen energy strategies: I. Current status and needs," Int. J. Hydrogen Energy, vol. 28, no. 3, pp. 229–236, 2003, doi: 10.1016/S0360-3199(02)00056-4.

[25] I. Dincer and C. Acar, "Review and evaluation of hydrogen production methods for better sustainability," Int. J. Hydrogen Energy, vol. 40, no. 34, pp. 11094–11111, 2015, doi: 10.1016/j.ijhydene.2014.12.035.
[26] M. A. Ahmadi, M. A. Rosen, and I. Dincer, "Greenhouse gas emissions and exergy of a solar-based multigeneration system," Energy Convers. Manage., vol. 88, pp. 833–846, 2014, doi: 10.1016/j.enconman.2014.09.024.
[27] M. Kanoglu, I. Dincer, and M. A. Rosen, "Understanding energy and exergy efficiencies for improved energy management in renewable energy systems," Renew. Sustain. Energy Rev., vol. 15, no. 4, pp. 1931–1942, 2011, doi: 10.1016/j.rser.2010.12.013.
[28] M. Mahmoudi, M. Yari, M. A. Rosen, and M. A. Amidpour, "Exergoeconomic analysis of a combined cycle power plant with a solar-assisted steam generator," Energy Convers. Manage., vol. 63, pp. 108–117, 2012, doi: 10.1016/j.enconman.2012.03.018.
[29] A. J. Wheeler and A. R. Ganji, Introduction to Engineering Experimentation, 3rd ed. London, U.K.: Pearson, 2010.
[30] B. E. Launder and D. B. Spalding, "The numerical computation of turbulent flows," Comput. Methods Appl. Mech. Eng., vol. 3, no. 2, pp. 269–289, 1974, doi: 10.1016/0045-7825(74)90029-2.
[31] H. K. Versteeg and W. Malalasekera, An Introduction to Computational Fluid Dynamics: The Finite Volume Method, 2nd ed. Oxford, U.K.: Elsevier, 2007.
[32] W. Chen, X. Zheng, and B. Liu, "3D numerical simulation and performance analysis of a micro-scale impulse steam turbine," Appl. Energy, vol. 185, pp. 1317–1325, 2017, doi: 10.1016/j.apenergy.2016.01.077.
[33] M. Rahimi, A. Asadi, and S. M. Khoshhal, "Computational fluid dynamics simulation and experimental validation of a micro steam turbine," Appl. Therm. Eng., vol. 111, pp. 1297–1306, 2017, doi: 10.1016/j.applthermaleng.2016.10.021.
[34] A. E. Kabeel, A. Khalil, Z. M. Omara, and M. M. Younes, "Theoretical and experimental parametric study of modified stepped solar still," Desalination, vol. 289, pp. 12–20, 2012, doi: 10.1016/j.desal.2011.12.023.
[35] V. K. Bhargava, P. K. Srivastava, and S. Kumar, "3D CFD modeling of a passive solar still and its experimental validation," Desalination, vol. 385, pp. 60–68, 2016, doi: 10.1016/j.desal.2016.02.016.
[36] T. Arunkumar, K. Raj, M. Chaturvedi, A. Thenmozhi, D. Denkenberger, and G. Tingting, "A review on distillate water quality parameter analysis in solar still," Int. J. Ambient Energy, vol. 42, no. 11, pp. 1335–1342, 2021, doi: 10.1080/01430750.2019.1587722.